

## Implementation of Spur Dikes to Reduce Bank Erosion of Temporary Diversion Channels During Barrages Construction

<sup>1</sup>Ali Talaat, <sup>2</sup>Karima Attia, <sup>3</sup>Gamal Elsaed, <sup>4</sup>Mohammad Ibraheem

<sup>1</sup>Department of Hydraulics and Irrigation, Ain Shams University

<sup>2</sup>Department of Hydraulics and Irrigation, Nile Research Institute, National Water Research Center.

<sup>3</sup>Department of Civil Engineering, Faculty of Engineering, Shobra, Banha University.

<sup>4</sup>Department of Civil Engineering, Faculty of Engineering, Shobra, Banha University.

**Abstract:** This study was initiated to introduce non-submerged spur dikes as training structures to reduce erosion at the opposite bank to diversion channel at Naga Hammadi barrage through minimizing the velocity values near the banks. The length of the bank to be protected is 450m. The width of diversion channel is 172m; however the average channel width at the region under study is 450m. A two dimensional mathematical model were used to simulate many cases. To assure model validity, experimental results were used for verification. The model simulated longitudinal and transverse velocities as well as the spur working length. A financial economic evaluation as a function of groin length is introduced to help in selecting the optimum group with minimum cost. Eighteen runs (18) were executed where three (3) effective parameters were tested. These parameters were the contraction ratio, which is defined as the spur length to the channel width (L/B), the spur orientation angle; and the spur spacing. The contraction ratio was varied between 0.1 and 0.2 while the used orientation angle are 60°, 90° and 120° and the spacing was 2, 4, and 7 times as much as the spur length. The measurements covered 60 grid points along four longitudinal lines (A, B, C, and D) crossed by 15 lateral cross sections. The study concluded that the maximum spur working length is occurred with repelling spurs of 120° with a 0.2 contraction ratio at 2L or 4L spacing. On the other hand, 7L spacing produced the minimum working length in addition to its discontinuity. It was also found that the working length is inversely proportional to the spur spacing but it is directly proportional to the spur length for a fixed orientation angle and spacing. The maximum and minimum values of longitudinal velocity occurred in the case of using a spur with an orientation angle of 90° with a contraction ratio of 0.2. It was also noticed that changing the spur length, spacing, and orientation angles did not affect the maximum transverse velocities. For the tested cases, the maximum and minimum transverse velocities are located at the middle third of the channel. There is a clear similarity between the longitudinal velocity in case of implementing repelling and straight spurs. For fixed spur length and spacing, using a group of spurs at any orientation angle, both longitudinal and transverse velocities decrease at the different cross sections in the vicinity of the bank by 50% and 20%, respectively. Using a group of 10% contraction ratio length presents more economic solution from the view of cost evaluation when compared to 20% contraction ratio length. The study recommended that 4 spur oriented at 60° with 10% contraction ratio length and spacing of 4 times spur length can be used to protect the attacked 450m at the bank facing the temporary diversion channel, while the repelling and straight types spur with 0.2 contraction ratio could be implemented to produce a deep channel. The scour associated to spurs existence is discussed in a separate paper.

**Key words:** Oriented Spur dike, mathematical model, velocity components, and working length.

### INTRODUCTION

In order to construct a regulating structure like a barrage, a temporary artificial channel of smaller width is established after which coffer dams or diaphragm walls are constructed to dewater the construction site to allow the workers and equipments to operate at the footings and the main skeleton of the barrage. After the closure of the construction site, the full surge of water way is diverted to the artificial channel. On the other hand, after opening the diversion channel the flow decelerates at the inlet due to the gradual contraction. However this phenomenon is reversed at the outlet due to the gradual enlargement. Consequently, the flow

**Corresponding Author:** Gamal Elsaed, Department of Civil Engineering, Faculty of Engineering, Shobra, Banha University

exits the diversion channel with high velocity to strike the opposite bank of the diversion channel thus causing its erosion. The implementation of spur dikes to minimize the impacts on the opposite bank of the diversion channel is investigated in this study. The spurs may be defined as a structure extending outward from the bank of a stream for the purposes of bank protection by deflecting the main current away from critical zones (Klingeman, P.C., S.M. Kehe, 1984). This research was thus initiated in order to define the optimum group of spurs that minimizing the bank erosion problem. Many parameters are involved to define the optimum group, the spur length, spacing, and orientation angles. The spur implementations cover bank length of 450 m, the number of spurs depends on the involved parameters especially spur length and spacing. The effect of these parameters on the flow pattern and velocities in the diversion channels is studied. A two dimensional finite element mathematical model was developed by Molinas and Hafez (2000) is used in this study.

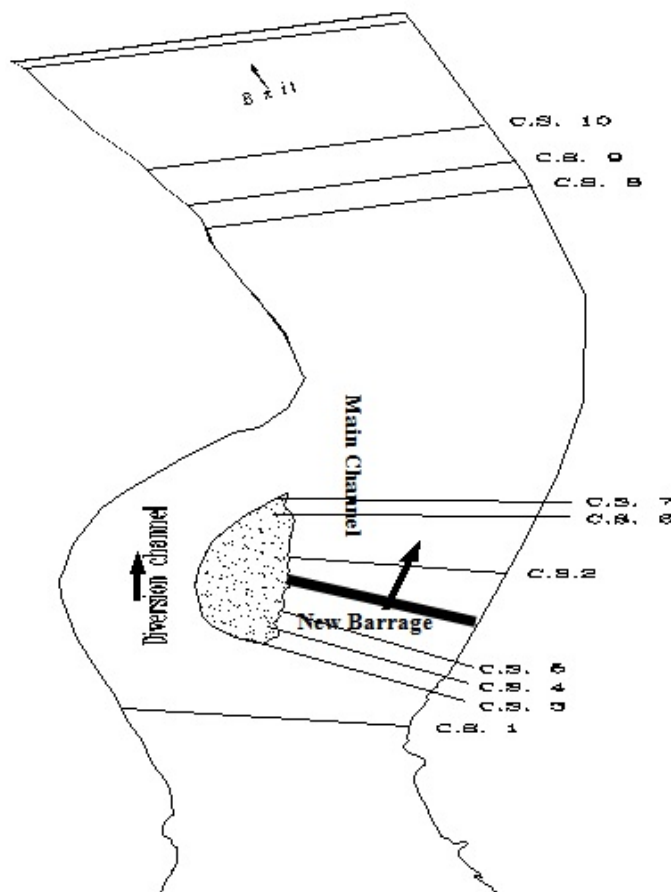


**Fig. 1:** General Layout

**Study Cases:**

A number of runs were simulated using the mathematical model; one of which represented the flow pattern without any spurs. This run was used as a reference to allocate the hydraulic performance of spur dike implementation at the opposite bank of the diversion channel. The runs names are formulated as spacing, function of spur type, and contraction ratio. For example,  $2A_{10}$  means that the spur spacing is equal to  $2L$  at a  $60^\circ$  (attracting spur) with 10% contraction ratio, and  $4S_{20}$  means that the spur spacing is equal to  $4L$  at a  $90^\circ$  (straight spur) with 20% contraction ratio, while  $7R_{10}$  means that the spur spacing is equal to  $7L$  at a  $120^\circ$  (repelling spur) with 10% contraction ratio. Moreover, the spur lengths corresponding to 10% and 20% contraction ratio are 45m and 90m respectively, as the average channel width is 450. It should be mentioned that in all the tested cases the group of groins covered a channel length of 450m. This was achieved by changing the number of groins to fit the assigned 450m according to spur length and spacing. Table 1 shows the number of groins used for each run and all other details related to spur length, spacing, contraction ratios and orientation angles.

**Table 1:** The Study Simulated Cases

Run Name	L/B	Number of Groins	Angle of Orientation	Spur Name
2A <sub>10</sub>	0.10	6	60°	Attracting
4A <sub>10</sub>	0.10	4		
7A <sub>10</sub>	0.10	3		
2A <sub>20</sub>	0.20	4		
4A <sub>20</sub>	0.20	3		
7A <sub>20</sub>	0.20	2		
2S <sub>10</sub>	0.10	6	90°	
4S <sub>10</sub>	0.10	4		
7S <sub>10</sub>	0.10	3		
2S <sub>20</sub>	0.20	4		
4S <sub>20</sub>	0.20	3		
7S <sub>20</sub>	0.20	2		
2R <sub>10</sub>	0.10	6	120°	Repelling
4R <sub>10</sub>	0.10	4		
7R <sub>10</sub>	0.10	3		
2R <sub>20</sub>	0.20	4		
4R <sub>20</sub>	0.20	3		
7R <sub>20</sub>	0.20	2		

**MATERIALS AND METHODS**

**Mathematical Model:**

The developed model governing differential equations are in the Cartesian X-Y coordinates, along and across the main flow direction, respectively. On the other hand, the Navier Stokes equations are used to describe motion. The fluid is assumed to be incompressible and follows a Newtonian shear stress law, whereby, viscous force is linearly related to the rate of strain. In the model, the hydrodynamics governing equations are the equations of conservation of mass and momentum. Conservation of mass equation takes the form of the continuity equation while Newton’s equations of motion in two dimensions express the conservation of momentum. The continuity equation is given as:

$$\frac{\partial U}{\partial X} + \frac{\partial V}{\partial Y} = 0 \tag{1}$$

The momentum equation in the longitudinal (X) direction is

$$U \frac{\partial U}{\partial X} + V \frac{\partial U}{\partial Y} = -\frac{1}{\rho} \frac{\partial P}{\partial X} + \frac{\partial}{\partial X} (2\nu_e \frac{\partial U}{\partial X}) + \frac{\partial}{\partial Y} (\nu_e (\frac{\partial U}{\partial Y} + \frac{\partial V}{\partial X})) + F_x + \left( \frac{\partial}{\partial z} \left( \frac{\tau_{fx}}{\rho} \right) \right)_{z=0} \tag{2}$$

The momentum equation in the lateral (Y) direction is

$$U \frac{\partial V}{\partial X} + V \frac{\partial V}{\partial Y} = -\frac{1}{\rho} \frac{\partial P}{\partial Y} + \frac{\partial}{\partial X} (\nu_e (\frac{\partial U}{\partial Y} + \frac{\partial V}{\partial X})) + \frac{\partial}{\partial Y} (2\nu_e \frac{\partial V}{\partial Y}) + F_y + \left( \frac{\partial}{\partial z} \left( \frac{\tau_{fy}}{\rho} \right) \right)_{z=0} \tag{3}$$

Where U = Longitudinal surface velocity, V = Transverse surface velocity, P = Mean pressure,  $\nu_e$  = Kinematics eddy viscosity,  $F_x$  = Body force in X direction,  $F_y$  = Body force in Y direction, g = Gravity acceleration, q = Average water surface slope,  $\rho$  = Fluid density,  $\tau_{fx}$  = Turbulent frictional stresses in X-direction,  $\tau_{fy}$  = Turbulent frictional stresses in Y-direction.

The assumptions used in the hydrodynamic model are:

- The density is assumed to be constant (incompressible fluid).
- Flow conditions are constant (discharge=2900m<sup>3</sup>/s).
- The turbulent viscosity varies with the velocity gradient.
- Two-dimensional surface analysis.
- Free surface as a rigid lid.
- Pressure is considered to be hydrostatic.
- Wind stresses are neglected.

It should be mentioned that complete details about numerical solution of the model governing equations, the boundary conditions and the working flow chart is presented in Ebraheem (2005).

**List of Symbols:**

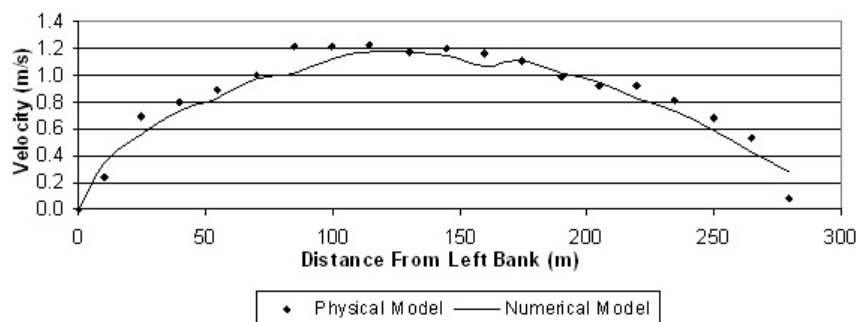
The following symbols are used in this paper:

L = Spur length	[m]
U = Longitudinal surface velocity	[m/s]
V = Transverse surface velocity	[m/s]
P = Mean pressure	[kg/m <sup>2</sup> ]
$\nu_e$ = Kinematics eddy viscosity	[m <sup>2</sup> /s]
$F_x$ = Body force in X direction = $g \sin \theta$	[kg.m/s <sup>2</sup> ]
$F_y$ = Body force in Y direction = 0.0	[kg.m/s <sup>2</sup> ]
g = acceleration due to gravity	[m/s <sup>2</sup> ]
S = spacing between spurs	[m]
q = Average water surface slope	[degrees]
r = Fluid density	[kg/m <sup>3</sup> ]
$\tau_{fx}$ = Turbulent frictional stresses in X-direction	[kg/m <sup>2</sup> ]
$\tau_{fy}$ = Turbulent frictional stresses in Y-direction	[kg/m <sup>2</sup> ]

**Model Testing, Validity and Verification:**

To verify the effectiveness of the numerical model for flow simulation, a previous experimental study, carried out in the Hydraulics Research Institute (HRI) Ministry of Water Resources and Irrigation, Egypt for Naga Hammadi Barrage, is used. A comparison between the numerical and physical results was achieved at two cross sections out of ten (cross section 6 and 7, at 50 m and 51.6 m respectively), from the experiment inlet, Figure 2. These 2 sections represent sections at 1500m and 1550m, respectively, in the field (prototype). The results are presented for a discharge of 1500m<sup>3</sup>/s. The figure indicates good agreement between the model results and the experiment data. This insures the capability of the current model to reproduce confident results.

**Cross Section No.6**



**Cross Section No.7**

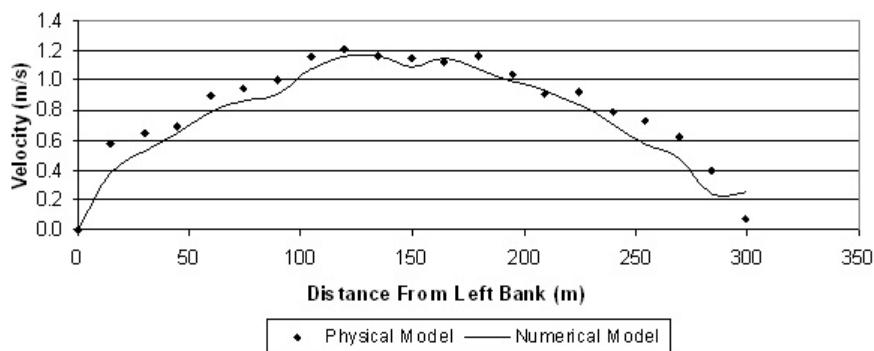


**Fig. 2: Testing the Validity of the Used 2-D Numerical Model**

## RESULTS AND DISCUSSION

The following sections show the results of the several executed simulations.

### *The Working Length:*

The spur working length is defined as the spur influence length which is extended upstream and downstream the spur location. To investigate the working length by the aid of velocity vectors, a finite element mesh was created. It consisted of more than 7200 measuring nodal which requires a long time in running the model. Figure 3 shows a part of the created mesh.

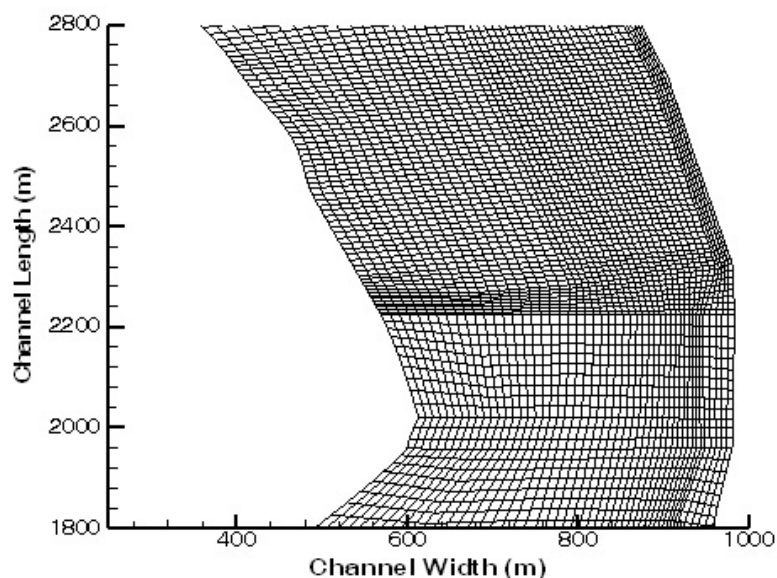


Fig. 3: Part of the Created Finite Element Mesh

The working length for a group of spurs is the summation of both separation point and reattachment lengths. Using a group of spurs may perform a continuous or separated working length. The continuous is the most favorable as it provides a weak region of flow in front of the bank that should be protected. This is shown in Figures 4 (a, b, and c) where the arrows define the velocity vectors in the channel.

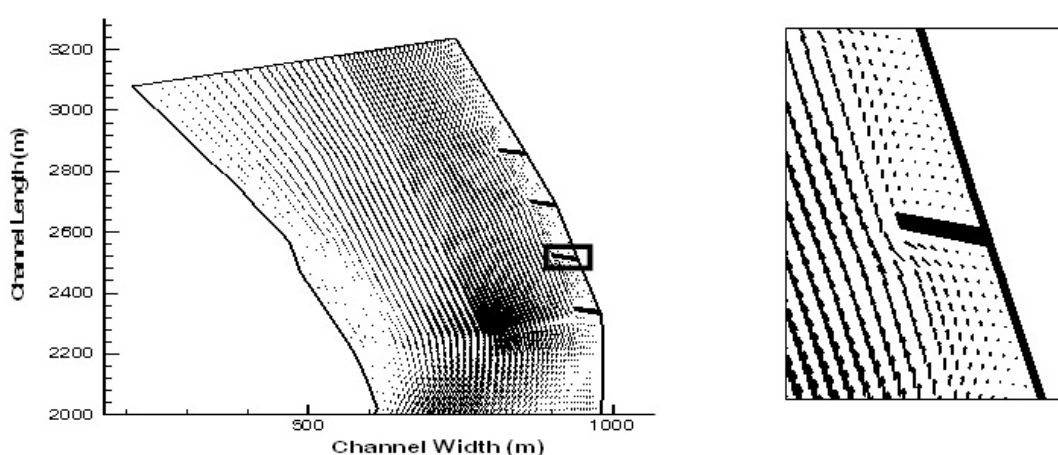
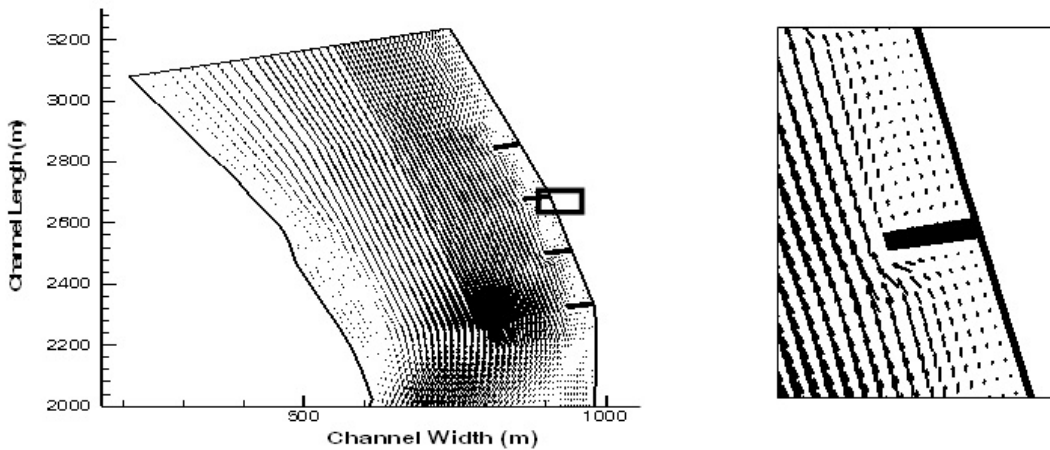
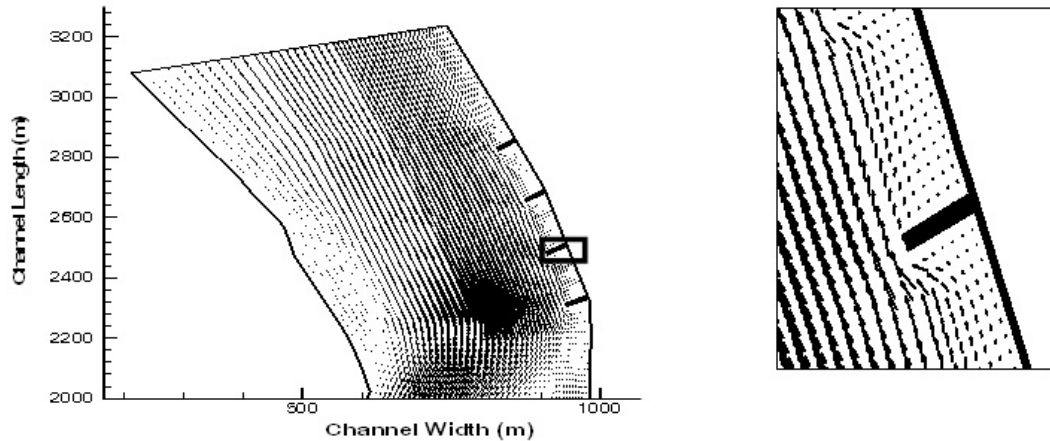


Fig. 4(a): Flow Pattern around Attracting Type Spur



**Fig. 4(b):** Flow Pattern around Straight Type Spur



**Fig. 4(c):** Flow Pattern around Repelling Type Spur

Table 2 summarizes the total working length for the different simulated cases. From the table it could be noticed that the maximum working length was obtained in case of implementing repelling spurs of 120° with 0.2 contraction ratio and 2L or 4L spacing. It could also be noticed that such spurs create a separation point length at the upstream in addition to the reattachment length at the downstream (which are the two components of working length). This agreed with what was concluded by Ebraheem (2005) and Attia (2006). It was also noticed that the working length is inversely proportional to the spacing between spurs. For fixed orientation angle and spacing, the working length is directly proportional to the spur length.

The above table illustrates that the working length was discontinuous, for all the simulated cases of spurs with spacing of 7L at any orientation angle and contraction ratio. From Table 2 it is noticed that the optimum groups for bank protection are 2A<sub>10</sub> and 2S<sub>10</sub> as they present the longest working length.

**Velocities:**

The importance of velocity in defining the optimum group of spurs for bank protection can not be neglected. The velocity is considered to be a focal parameter for flow characteristics which helps to indicate the positions of scour and deposition due to spurs existence. The velocity was measured at 60 locations distributed along four lines in the longitudinal direction and at 15 cross sections, 40m apart. It should be mentioned that the longitudinal lines (A and B) are distributed to cover the channel width in order to define the flow pattern in the vicinity of spurs. As for line C and D, they are used to define the behavior of the velocity at the middle of the channel and at the opposite bank, respectively, Table 3 and Figure 4. It should be mentioned that line (A) is located prior to groin tip by 5m and 50m for group with 10% and 20% contraction ratio respectively. However line (B) is located prior to groin tip by 10m only for the group of 20% contraction ratio.

**Table 2:** The Working Length and Its Continuity

Run Name	Working Length (m)	Working Length Function in Length (L)	Continuity of Working Length
Basic	-----	-----	-----
2A <sub>10</sub>	537.25	11.939	£
4A <sub>10</sub>	332.58	7.391	£
7A <sub>10</sub>	220.02	4.889	X
2A <sub>20</sub>	537.25	5.969	£
4A <sub>20</sub>	496.32	5.515	X
7A <sub>20</sub>	250.72	2.786	X
2S <sub>10</sub>	537.25	11.939	£
4S <sub>10</sub>	383.75	8.528	£
7S <sub>10</sub>	235.37	5.230	X
2S <sub>20</sub>	527.02	5.856	£
4S <sub>20</sub>	527.02	5.856	X
7S <sub>20</sub>	220.02	2.445	X
2R <sub>10</sub>	511.67	11.37	£
4R <sub>10</sub>	378.64	8.414	£
7R <sub>10</sub>	204.67	4.548	X
2R <sub>20</sub>	614.01	6.822	£
4R <sub>20</sub>	614.01	6.822	X
7R <sub>20</sub>	163.73	1.819	X

**Table 3:** The Distance between Right Bank and Measuring Lines after Diversion Channel

Line	A	B	C	D
Distance From Right Bank (m)	40	80	200	420

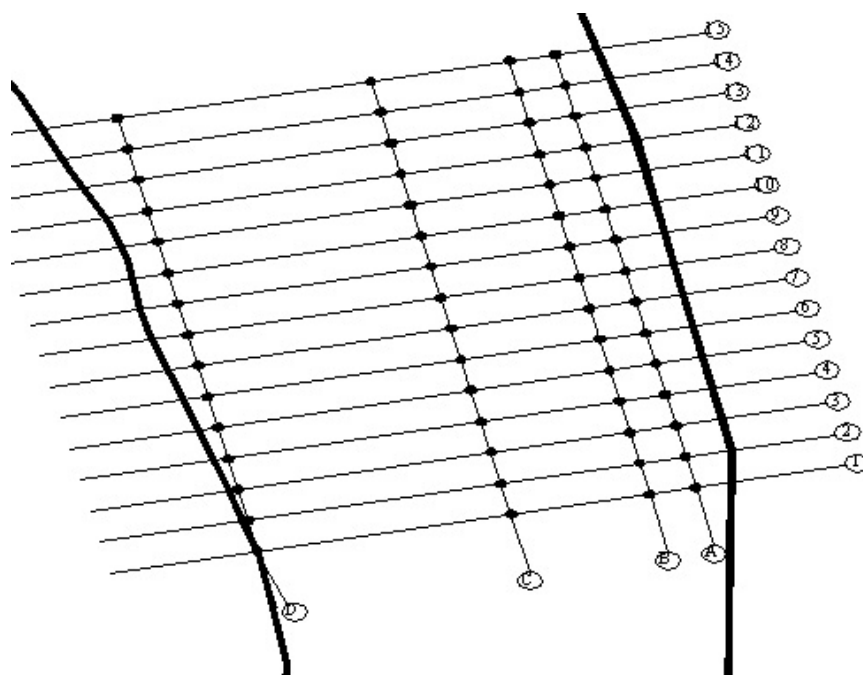


**Fig. 5:** Location of Velocity Measurements

A summary of the obtained velocity values resulted from the different simulations is presented in tables 4 and 5, where the maximum and minimum longitudinal and transverse velocities are given for each run together with their locations with respect to the cross section number and line symbol.

**Longitudinal Velocity:**

Table 4 shows that the maximum and minimum longitudinal velocity ( $U_{max}$ , and  $U_{min}$ ) that occurred when using a 90° (straight spur) with 20% contraction ratio. These results are in agreement with the results obtained by Attia (2006). That assures the fact that using straight spurs with long lengths, with spacing 4L or less, makes the group of spurs acting as a firewall against flow which, by its turn, decrease the width of channel and increase the velocity at the middle of the channel and the opposite bank, to the erected spurs, as well. This

**Table 4:** Locations of the Maximum and Minimum Longitudinal Velocities

Run Name	Max. U (m/s)	Location		Min. U (m/s)	Location	
		Line	X-Sec		Line	X-Sec
Basic	2.433	C	1	-0.122	D	5
2A <sub>10</sub>	2.394	C	1	-0.105	D	5
4A <sub>10</sub>	1.929	C	1	-0.073	D	4
7A <sub>10</sub>	2.417	C	1	-0.112	D	5
2A <sub>20</sub>	2.446	C	1	-0.141	A	6
4A <sub>20</sub>	2.443	C	1	-0.162	A	6
7A <sub>20</sub>	2.423	C	1	-0.168	A	6
2S <sub>10</sub>	2.391	C	2	-0.100	D	4
4S <sub>10</sub>	2.394	C	2	-0.107	A	8
7S <sub>10</sub>	2.412	C	1	-0.109	D	5
2S <sub>20</sub>	2.479	C	1	-0.154	A	9
4S <sub>20</sub>	2.482	C	1	-0.163	A	14
7S <sub>20</sub>	2.461	C	1	-0.175	A	5
2R <sub>10</sub>	2.398	C	2	-0.104	D	6
4R <sub>10</sub>	2.407	C	1	-0.107	D	4,5
7R <sub>10</sub>	2.421	C	1	-0.112	D	5
2R <sub>20</sub>	2.464	C	1	-0.131	A	8
4R <sub>20</sub>	2.434	C	1	-0.152	A	13
7R <sub>20</sub>	2.433	C	2	-0.101	D	5
7S <sub>10</sub>	2.412	C	1	-0.109	D	5

**Table 5:** Locations of the Maximum and Minimum Transverse Velocities

Run Name	Max. V (m/s)	Location		Min. V (m/s)	Location	
		Line	X-Sec		Line	X-Sec
Basic	0.375	C	1	-0.638	C	14
2A <sub>10</sub>	0.302	C	1	-0.605	C	12
4A <sub>10</sub>	0.237	C	1	-0.497	C	13
7A <sub>10</sub>	0.340	C	1	-0.652	C	12
2A <sub>20</sub>	0.126	C	1	-0.631	C	10
4A <sub>20</sub>	0.145	C	1	-0.632	C	12
7A <sub>20</sub>	0.160	C	1	-0.657	C	15
2S <sub>10</sub>	0.280	C	1	-0.598	C	11
4S <sub>10</sub>	0.299	C	1	-0.626	C	12
7S <sub>10</sub>	0.325	C	1	-0.670	C	12
2S <sub>20</sub>	0.112	C	1	-0.632	C	10
4S <sub>20</sub>	0.087	C	1	-0.672	C	11
7S <sub>20</sub>	0.111	C	1	-0.729	C	15
2R <sub>10</sub>	0.299	C	1	-0.592	C	12
4R <sub>10</sub>	0.317	C	1	-0.625	C	13
7R <sub>10</sub>	0.342	C	1	-0.648	C	12
2R <sub>20</sub>	0.133	C	1	-0.625	C	10
4R <sub>20</sub>	0.183	C	1	-0.768	C	11
7R <sub>20</sub>	0.226	C	1	-0.811	C	15

is used to maintain deep channels that are used in navigation processes. In fact this is one of the main purposes of using spurs. This agrees with the results concluded by Ebraheem (2005), as well. The table also illustrates that for all simulated cases, the maximum longitudinal velocities are directly proportional to the spur length and is located at the middle third of the channel along line C (200m from right bank), especially, at cross sections 1 and 2 at the most contracted region (after the flow exits the diversion channel).

From Table 4 it is noticed that the group of 4A<sub>10</sub> presents the optimum condition for bank protection as it presents the minimum values for both maximum and minimum longitudinal velocities when compared to the other cases. Also, it should be mentioned that the longitudinal velocity dominates the scour holes associated to existence of groins, in other words it can be said that the group of 4A<sub>10</sub> presents minimum bed morphological changes. The investigated spacing agrees with what obtained by Mosselman (2000).

**Transverse Velocity:**

The maximum transverse velocities are slightly affected by changing the spur length, spacing, and orientation angles, as shown in Table 5. However for all simulated cases, the maximum and minimum transverse velocities are located at the middle third of the channel. This could be attributed to the fact that as the flow exits the diversion channel, it impacts the right bank. This causes the flow, in behind, to be diverted away from that region. This also explains the negative value of the minimum transverse velocity. It was also



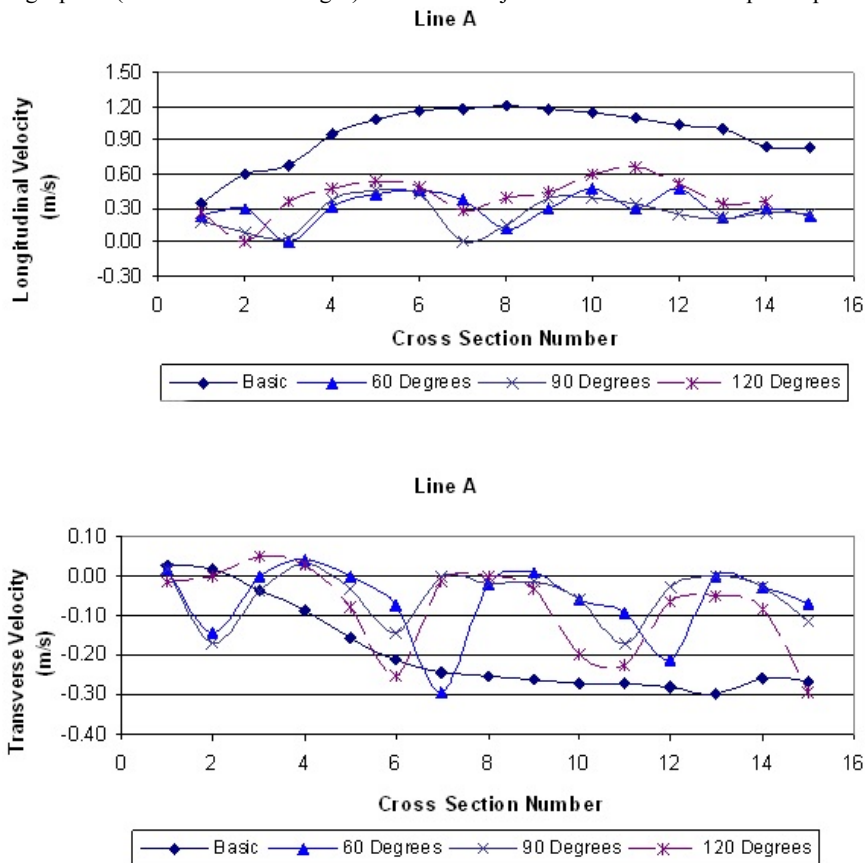
noticed that, for all the simulated cases, the repelling group of spurs has higher values of the maximum transverse velocities than that in cases of using straight and attracting groups. This means that larger and deeper scour holes will occur in front of spurs. Moreover, large amounts of downstream sediment occur due to the dead zone of weak flow presented in terms of velocity. In other words, it can be said that scour holes are inversely proportional to the orientation angle measured from the downstream. This agrees with the results obtained by Melville (1992). The table also shows that for all simulated cases, the maximum values of transverse velocity are inversely proportional to the spur length and are directly proportional to the spacing between spurs.

From Table 5 it is noticed that the group of  $4A_{10}$  presents the average values for both maximum and minimum transverse velocities which is valuable in preventing deposition of the facing bank of groins erection.

**Effects of the Orientation Angles on Velocities:**

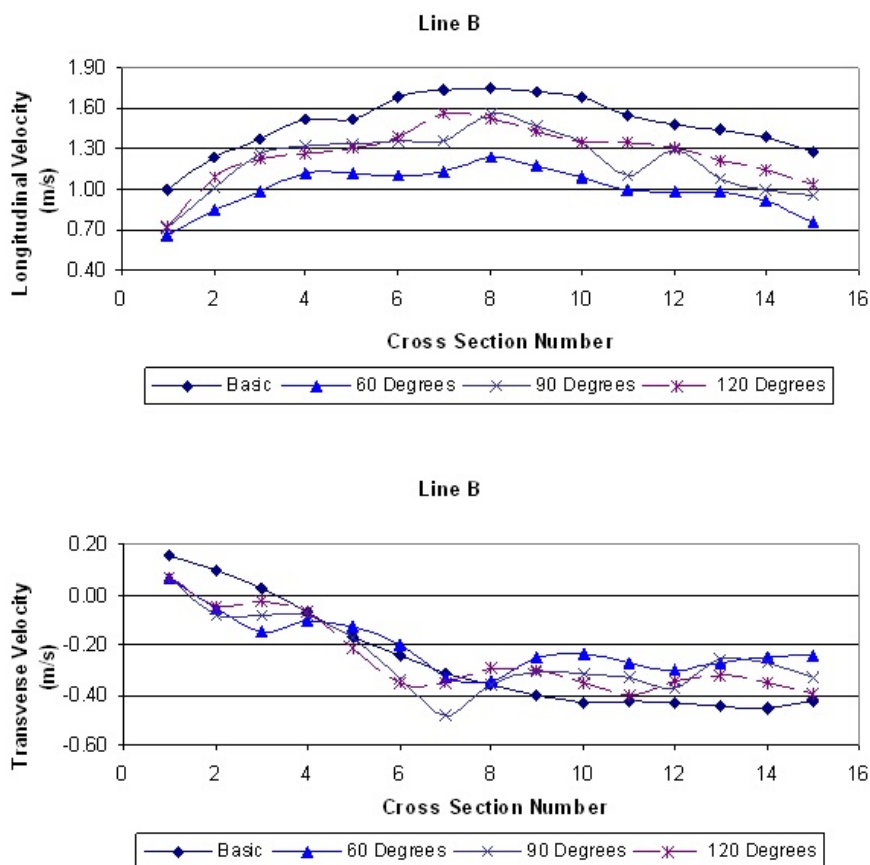
To test the effect of the orientation angles on the flow pattern, the relationships between the velocity and the orientation angles are plotted for the basic case and the simulated cases along the different lines. The contraction ratio was kept constant during this investigation. The ratio 0.10 with spacing of 4L was selected. This ratio was chosen based on different simulated cases. This ration is the most effective influencing parameter.

Figure 6 illustrates that at line (A) there is a clear similarity in the trend of both the longitudinal and transverse velocities. However, using a group of spurs at any orientation angle decreases the longitudinal and transverse velocities by 50% and 20% respectively, at the different cross sections when compared to basic case. As for the peak values of the longitudinal velocities, for the repelling group ( $120^\circ$  orientation angle), they were slightly higher at most of the cross sections. On the other hand, the peak values of the transverse velocity, for the attracting spurs ( $60^\circ$  orientation angle) are located just downstream the tip of spur.



**Fig. 6:** Longitudinal and Transverse Velocities at Line (A) for 0.1 Contraction Ratio and 4L Spacing For Different Orientation Angles

From Figure 7, it can be seen that the longitudinal and transverse velocities, for line B (80m from right bank), with attracting spurs showed lower values than in case of repelling and straight spurs while both the repelling and straight spurs have almost equal values. However, using spurs at an angle to the bank improves the situation, relative to the basic case, as it decreases the erosive velocity in the vicinity of the right bank. From the figure, it can also be concluded that the longitudinal velocity is directly proportional to the orientation angle. However, the transverse velocity, using spurs, does not noticeably change relative to the basic case.



**Fig. 7:** Longitudinal and Transverse Velocities at Line (B) for 0.1 Contraction Ratio and 4L Spacing For Different Orientation Angles

At the middle of the cross section of the channel, along line (C), the longitudinal and transverse velocities show the same trend relative to the basic case using different orientation angles. However, for the case of the attracting spurs, lower values of longitudinal velocities, relative to the basic case, were observed. On the contrary, the repelling and straight spurs gave the greater values relative to the basic case. This means that repelling and straight spurs maintain deep channel for navigational purposes more than the attracting spurs. Moreover it was noticed that the tested orientation angles had the same trend and value of the transverse velocity, relative to the basic case. Also, it is noticed that the group of 4A<sub>10</sub> presents the best solution to disperse the velocity away from the attacked bank.

At line (D), along the opposite bank, the longitudinal and transverse velocities for the tested cases show the same trend relative to the basic case. It should also be mentioned that the tested cases have higher values relative to the basic case and are directly proportional to the cross section from the point of view of the longitudinal velocity. On the contrary, the transverse velocities, for all the tested cases, are lower relative to the basic case. They are also inversely proportional to the cross section. In addition to that, the longitudinal velocity, in case of the attracting spurs, has a higher value than in case of the tested repelling or straight spurs. The attracting group presented in 4A<sub>10</sub> proves effective performance in preventing the deposition at the opposite bank.

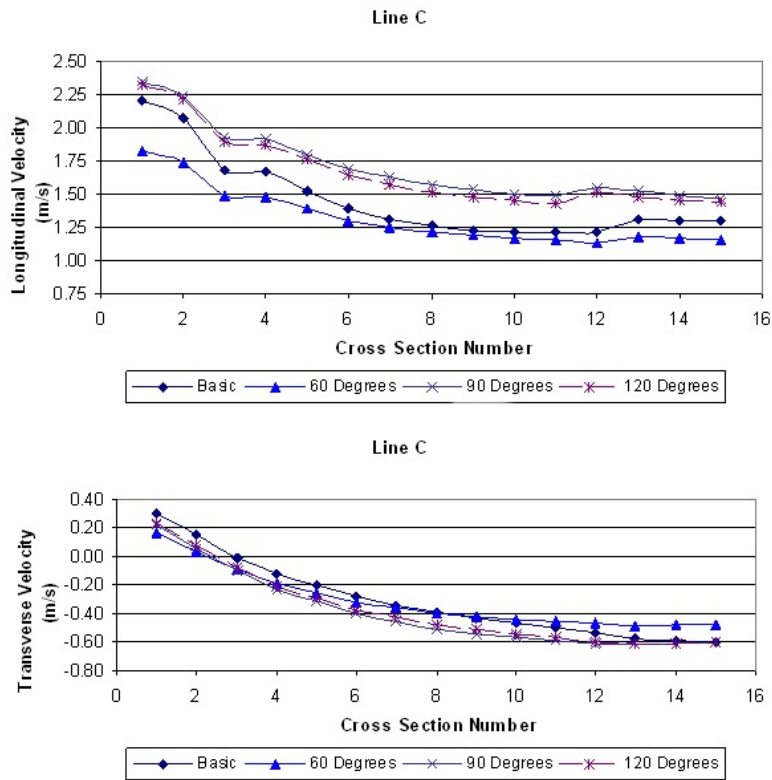


**Fig. 8:** Longitudinal and Transverse Velocities at Line (C) for 0.1 Contraction Ratio and 4L Spacing For Different Orientation Angles

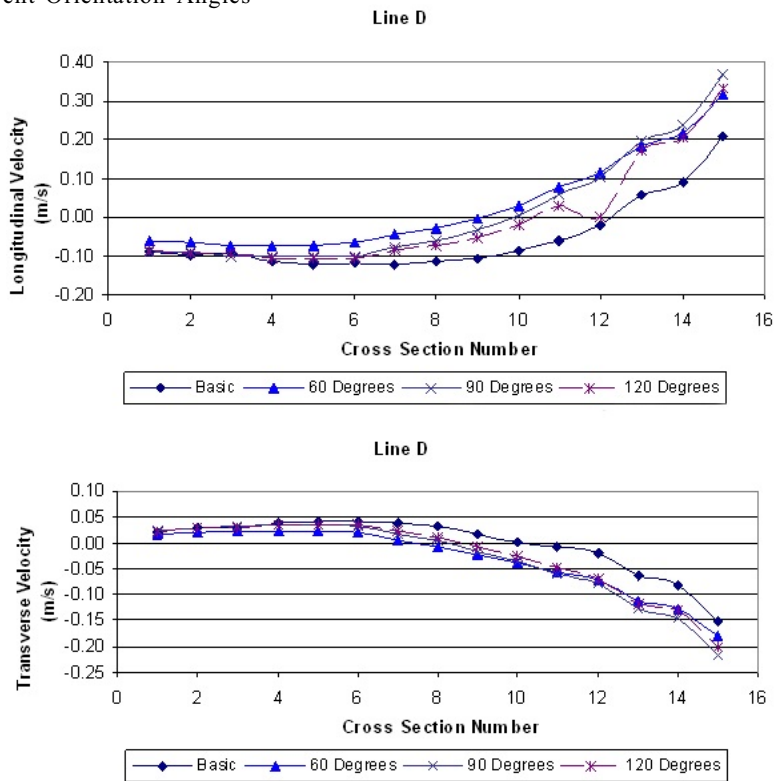


**Fig. 9:** Longitudinal and Transverse Velocities at Line (D) for 0.1 Contraction Ratio and 4L Spacing For Different Orientation Angles

Tables 6 and 7 summarize the average longitudinal and transverse velocities, respectively, for a group of spurs with 10% contraction ratio and 4L spacing at different orientation angles and velocity lines. Also, the percentage of reduction or increase relative to the basic case is given in the same table. It should be noted that the negative sign refers to the reduction in value.

**Table 6: Average Longitudinal Velocities at Different Orientation Angles**

Angle Line	Average Longitudinal Velocities (m/s)				% Basic Case		
	Basic	60°	90°	120°	60°	90°	120°
A	0.956	0.297	0.253	0.391	-68.933	-73.536	-59.100
B	1.492	1.005	1.21	1.261	-32.641	-18.901	-15.483
C	1.459	1.321	1.712	1.669	-9.459	17.341	14.393
D	-0.053	0.03	0.014	-0.006	156.604	126.415	88.679

**Table 7: Average Transverse Velocities at Different Orientation Angles**

Angle Line	Average Longitudinal Velocities (m/s)				% Basic Case		
	Basic	60°	90°	120°	60°	90°	120°
A	-0.19	-0.062	-0.051	-0.082	-67.368	-73.158	-56.842
B	-0.26	-0.204	-0.249	-0.251	-21.538	-4.231	-3.462
C	-0.306	-0.311	-0.391	-0.373	1.634	27.778	21.895
D	-0.002	-0.032	-0.031	-0.025	1500	1450	1150

From the above tables, it can be concluded that, at most of the velocity lines, both repelling and straight spurs have approximately similar values of transverse velocity. Line (C) represents the impact of spur implementation on the velocity at the middle of the channel. The attracting spurs (60°) reduced the average longitudinal velocity, while the straight and repelling spurs produced greater values relative to the basic case. Therefore, implementing repelling spurs will be useless as it couldn't create a slack flow upstream, while the attracting group of 4A<sub>10</sub> acts efficiently at the attacked bank. It maintains the depth at the middle of the channel and prevents the deposition at the left bank. Also, it should be mentioned that using the group of 4A<sub>10</sub> decreases the velocity in the vicinity of the 450m eroded bank by approximately more than 65% as an average value. As for straight spurs, they can be used for the purposes of bank protection and to increase the depth at the middle of channel for navigational aims.

**Cost Evaluation Test:**

The total number of groins in each simulation case plays an important role in choosing the optimum solution for minimizing bank erosion problem in the diversion channel. The number should provide enhancement in bank protection, at the same time the construction cost should be reasonable taking into account a fewer numbers of groins never refers to lower cost. The total number of groins is a function of groin length and spacing such to cover the 450m from the bank under study. In other words, the total number of groins is inversely proportional to groin length and spacing. As the angle of orientation doesn't impact on the number of groins; in Figure 10, the symbols A, S, and R are replaced by symbol (G). The present cost evaluation test for the simulated cases is a rough estimation for cost as it's presented as a function of total length for different runs. The total length is presented by multiply the groin length by number of groins for each case.

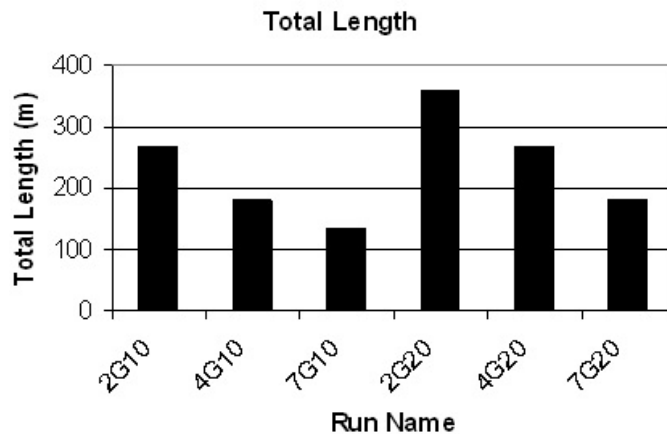


**Fig. 10: Total Length of Groins for Different Simulation Cases**

Combining Table 1 and Figure 10 clearly indicates that, the maximum length was found for the group of 20% contraction ratio and 2L spacing; however the number of groins for that group is 3 which isn't the maximum one that indicates the higher cost. Moreover, using a group of 10% contraction ratio length presents more economic solution when compared to 20% contraction ratio length. After discussing the technical parameters of working length and continuity clearly was that, for different orientation angles, only the groups of 10% length with 2 and 4L spacing was technically succeeded in bank protection. However, the group of 4L spacing had the most economical cost.

#### **Conclusion and Recommendations:**

This research investigated the effect of spur installation on different parameters. For the working length it was found that using repelling spurs (120° with 0.20 contraction ratio with spacing less than 4L) produced the longest working length. However to keep the working length continuous it is preferred to use spurs with length less than 10% of the channel width with spacing less than 4L. It was found that the maximum velocity for the tested cases is similar to the basic case velocity. On the other hand, using attracting spurs (0.10 contraction ratio and 60° orientation angle with spacing of 4L) proved to be the best case for bank protection and sedimentation processes. All maximum longitudinal velocities are located at the middle third of the channel and all minimum longitudinal velocities are located near the channel sides. The maximum and minimum transverse velocities are located at the middle third of the channel; also the maximum values of transverse velocities are inversely proportional to spur length and are directly proportional to the spacing between the spurs. For fixed spur length and spacing, it was found that using a group of spurs at any orientation angle decreases the velocity at the different cross sections in the vicinity of the bank by 50% and 20%, for the longitudinal and transverse velocities respectively. At the middle of channel it was found that only the attracting spurs show lower values than the basic case for longitudinal velocities, while at the opposite bank of erection it was found that the tested cases have higher values than the basic case. This means that using attracting spurs is protecting the bank optimally due to the impact of diversion channel. However both repelling and straight spurs maintain deep channel. However, testing the economic cost proved that this case is not the least cost from the economical point of view. The study recommended that similar study should be conducted using submerged spurs rather than emerged spurs. A checklist should be created after simulating more cases to define the suitability of each type according to the tackled problems. A complete economical study should be conducted and evaluated relating to the optimum technical evaluations.

#### **REFERENCES**

- Attia, K.M. and G. Elsaid, 2006. "The Hydraulic Performance of Oriented Spur Dike Implementation in Open Channel" Paper presented to Tenth International Water Technology Conference, Egypt.
- Ebraheem, M.M.M., 2005. "Hydrodynamic Behavior of Bank Protection Structures (Groins)" Thesis Submitted to Faculty of Engineering, Banha University for partial Fulfillment of the Requirements for Master Degree of Science in Civil Engineering (Irrigation & Hydraulics), Egypt, November.
- Klingeman, P.C., S.M. Kehe and Y.A. Owusu, 1984. Stream Bank Erosion Protection and Channel Scour Manipulation Using Rock Fill Dikes and Gabions, (No. WRR-98), Oregon state University, Water Resources Research Institute, Corvallis, Oregon, USA.
- Molinas, A. and Y.I. Hafez, 2000. "Finite Element Surface Model for Flow around Vertical Wall Abutments", *Journal of Fluid and Structures*, 14: 711-733.
- Mosselman, E., 2000. Technical Memorandum on Groyne Length and Spacing, Delft Hydraulics Lab. Communication, Delft, The Netherlands.
- Melville, B.W., 1992. "Local Scour at Bridge Abutment", *Journal of Hydraulic Engineering*, 118(4): 615-631.